The validity of the Neumann–Kopp rule[1]

Emília Illeková[1], Jean-Claude Gachon[2], Jean-Jacques Kuntz[2]

[1]Institue of Physics, Slovak Academy of Sciences, Dúbravská cesta 9, SK-842 28 Bratislava, Slovakia
[2]UMR 7555, Groupe Thermodynamique et Corrosion, Université Henri Poincaré, Nancy 1, BP 239, F-54506 Vandoeuvre-lès-Nancy, Cedex, France
Email: fyziille@savba.sk, Jean-Claude.Gachon@lcsm.uhp-nancy.fr

Abstract

Molar heat capacities at constant pressure of $Al_{90}Fe_7Nb_3$ master alloy and both as-quenched and crystallized ribbons were determined by the step-by-step method using differential scanning calorimetry from 310 to 1080 K. The experimental temperature dependencies have been analytically fitted by polynomial $C_p(T) = a + bT + cT^2 + dT^{-1} + eT^{-2}$. The $a - e$ polynomial parameters have also been physically appraised and correlated with the measurements. The validity of the Neumann-Kopp rule relating the heat capacities of the multiphase $Al_{90}Fe_7Nb_3$ alloy and its three equilibrium phases, namely Al, Al_3Fe and Al_3Nb, has been tested.

1 Introduction

During the workshop Thermophysics 2001 [1], the step-by-step differential scanning calorimetry was introduced. The reproducibility and uncertainty of the molar heat capacity data under normal pressure, $C_p(T)$, for metal standards were tested. The temperature dependence of $C_p(T)$ for one compound was determined and fitted by polynomial from 310 to 1473 K.

In this paper, the $C_p(T)$ measurements of the bulk multiphase $Al_{90}Fe_7Nb_3$ master alloy and also the as-quenched and crystallized ribbon up to 1080 K is presented. The molar heat capacities of the heterogeneous bulk and ribbon alloys are related to the heat capacities of their phases.

The rapidly quenched Al-based intermetallics are interesting new materials because of their heterogeneous amorphous or nanocrystalline microstructures and associated outstanding mechanical properties.

2 Experimental

2.1 Preparation of samples

The fcc-Al of 99.999% purity used was a standard. The monoclinic-Al_3Fe, tetragonal-Al_3Nb compounds and $Al_{90}Fe_7Nb_3$ master alloy, were prepared by induction melting of Al, Fe and Nb elements of 99.9% purity in an argon atmosphere, homogenized and cooled from 1523 K to ~ 423 K at 10^2 K s^{-1}. Ribbons (20 μm thick and ~10 mm wide) were produced by planar flow-casting of the melt from 1600 K at 10^6 K s^{-1} in air. The

[1] E. Illeková, J.C. Gachon, J.J. Kuntz: The validity of the Neumann-Kopp rule. Thermophysics 2002. Meeting of the Thermophysical Society Working Group of the Slovak Physical Society, October 24-25, 2002, Kočovce, Slovakia, Ed.: Libor Vozár, Constantine the Philosopher University in Nitra Faculty of Natural Sciences 2002, p. in press.

inductively coupled plasma spectroscopy (ICPS) analysis determined the true chemical composition of the alloy to be $Al_{91.5}Fe_{6.8}Nb_{1.7}$ (±1 % of element content). X-ray diffraction patterns were obtained by standard XRD using CuK_α radiation. The homogeneity and equilibrium structures of both compounds were confirmed. In the case of the master alloy and the heat treated to 1100 K ribbon, the equilibrium phases fcc-Al, monoclinic-Al_3Fe (C_{2h}^3 symmetry) and tetragonal-Al_3Nb (D_{4h}^{17} symmetry) were identified and also few unidentified diffraction lines were observed. No oxides were present. In the case of the as-cast ribbon, no crystalline phases were detected either by X-ray or transmission and scanning electron microscopy (TEM and SEM).

2.2 Differential scanning calorimetry: step-by-step heat capacity measurements

The heat capacities at constant pressure, $\boldsymbol{C_p}$, (an overall uncertainty ±5%), were determined in 10 K steps between 310 and 1080 K, except for Al sample with lower melting, with a Setaram DSC-111, designed as a Calvet type calorimeter. Samples of about 0.09-0.36 g, alumina crucibles and an Ar atmosphere were used. The heating rate was 3 K min^{-1} for 200 s and then the temperature was kept steady for 400 s. So, while an overall heating rate was 1 K min^{-1}, the steady state in the samples could be realized in each temperature step (except the transformation regions giving the anomalous artifacts). The complete procedure has been described in [1].

No appreciable oxidation, weight losses or reactions between samples and the alumina laboratory crucible were observed at the end of the measurements.

2.3 Curve fitting procedure

The classical polynomial tendency (1) for $C_p(T)$ of metals is recommended in [2].

$$C_p = a + bT + cT^2 + dT^{-1} + eT^{-2}. \quad (1)$$

It has been used instead of the theoretical temperature dependence of solids [3]

$$C_p = C_{har} + [\frac{2\pi^2}{3} N_A N(E_F) k_B^2 + 3\beta\gamma_G R]T + \frac{2\pi^2}{3} N_A N(E_F) k_B^2 \beta\gamma_G T^2 +$$

$$+ \beta\gamma_G N_A k_B \exp\{\frac{S_{vac}}{k_b}\} \frac{E_{vac}^2}{k_B^2} \exp\{-\frac{E_{vac}}{k_B T}\} T^{-1} + N_A k_B \exp\{\frac{S_{vac}}{k_B}\} \frac{E_{vac}^2}{k_B^2} \exp\{-\frac{E_{vac}}{k_B T}\} T^{-2}. \quad (2)$$

$C_{har} = 3R$ is the harmonic vibrations heat capacity, N_A, R and k_B are the Avogadro, gas and Boltzmann constants, β is the cubic expansion coefficient, γ_G is the thermodynamic Grüneisen parameter, $N(E_F)$ is the electron density of states at the Fermi level, E_{vac} and S_{vac} are the vacation formation enthalpy and entropy.

The polynomial coefficients a, b, c, d and e were found by the Simplex least-squares minimization procedure.

3 Results and discussion

The heat capacity of an as-prepared sample is, in general, uses to be slightly different from that of the heat-treated samples probably because of some irreversible anharmonic effects. Checked by successive runs on the well-relaxed metallic samples, the reproducibility of the step-by-step method data of C_p is ± 0.1 J K^{-1} mol^{-1}.

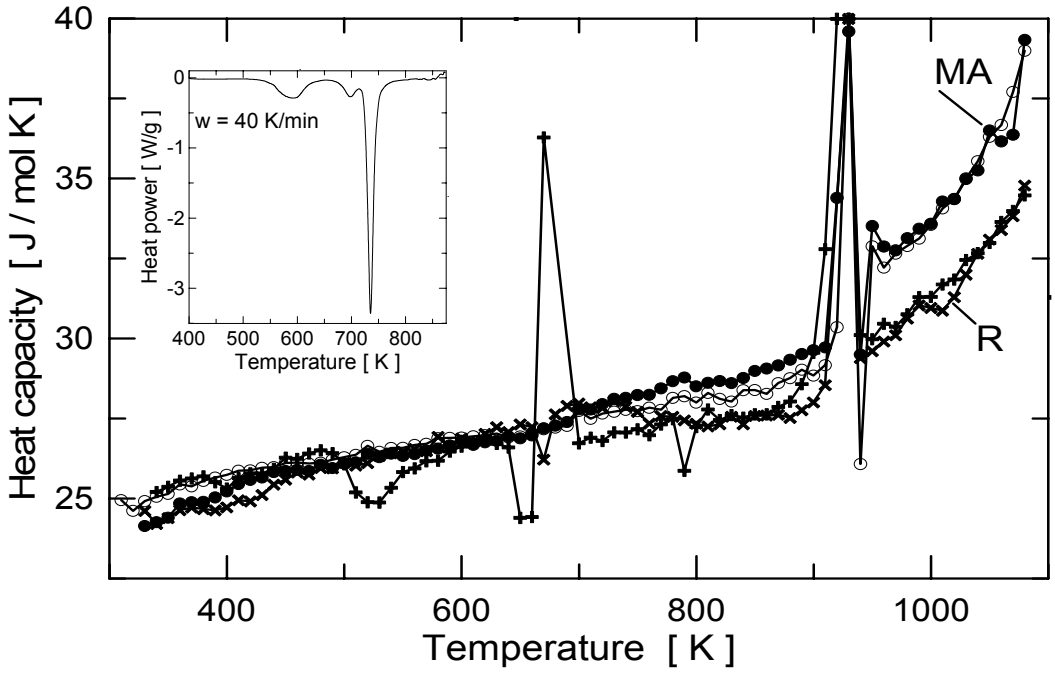

Fig 1 Experimental molar heat capacities of as-prepared (o) and relaxed by heating to 1080 K (•) $Al_{90}Fe_7Nb_3$ master alloy and as-quenched (+) and partially melted by heating to 1080 K (×) ribbon vs. temperature. The inset shows the DSC curve of the as-quenched ribbon [4].

Fig. 1 presents the experimental points of the molar heat capacity for both as-prepared and heat-treated master alloy and ribbon samples. The irregularities in the *Cp(T)* dependence below 900 K correlate well with the configurational contributions of the four step crystallization in the as-quenched ribbon as can be confirmed by the differential scanning calorimetry (DSC). A pronounced anomaly just above 900 K is due to the melting of aluminium in all samples. The otherwise monotonous reproducible *Cp(T)* of the heat-treated master alloy and ribbon samples was a subject for the following analyses.

The X-ray diffraction patterns established that both the master alloy and the heat-treated ribbon are mixtures of the same equilibrium phases [5]. Therefore, namely fcc-Al, monoclinic-Al_3Fe and tetragonal-Al_3Nb have been prepared and measured. Fig. 2 presents the experimental points of *Cp(T)* for the phases. They do not depart from the classical polynomial tendency (1), which in the case of the intermetallics is extremely weak (excepting a defect reflecting the melting of 1.4 at % of the Al-based impurity in Al_3Nb). On the contrary, the $C_p(T)$ of α-Al presents a large anharmonic contribution, a fact which has already been tabulated [6]. Assuming $a = 3R$, $b > 0$ and d/e = const (following eq. (2)), the ideal polynomial fits for the phases were analytically determined and they are also in Fig.2. The ideal polynomial parameters are in the Tab.1.

Knowing the five material parameters, namely β, γ_G, $N(E_F)$, E_{vac} and S_{vac} the true polynomial (1) parameters $a - e$ might be calculated. Assuming that $\beta = 3\ \alpha = 3x2.87x10^{-5}\ K^{-1}$ for Al and also both trialuminides, where α is the coefficient of linear expansion of Al [7], $\gamma_G = 2/3$ for Al and 1 for both trialuminides [3] and $N(E_F) = 0.36$, 0.21 and 0.17 $eV^{-1}\ at^{-1}$ [8], polynomial parameters b, c and d/e and $a = 3R$ (see Table 1)

were theoretically appraised. Accepting the ±5% overall uncertainty of the experimental data, the physically real parameters were analytically deduced (see tab.1) using the appraised parameters as the initial values for the iterative fitting.

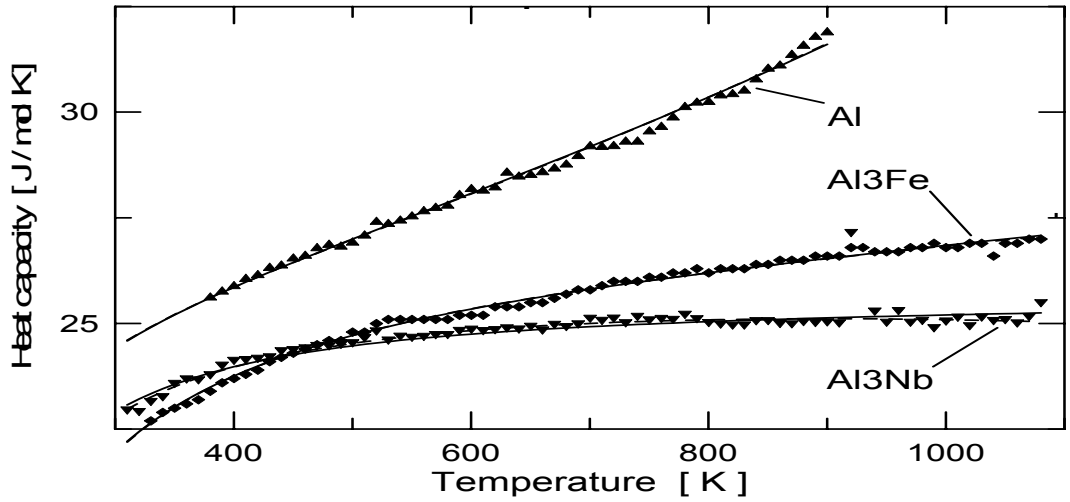

Fig 2 Temperature dependence of molar heat capacities of α-Al (▲), monoclinic-Al_3Fe (♦) and tetragonal-Al_3Nb (▼). Ideal (- - - -) and physically real (——) polynomial (1) fits.

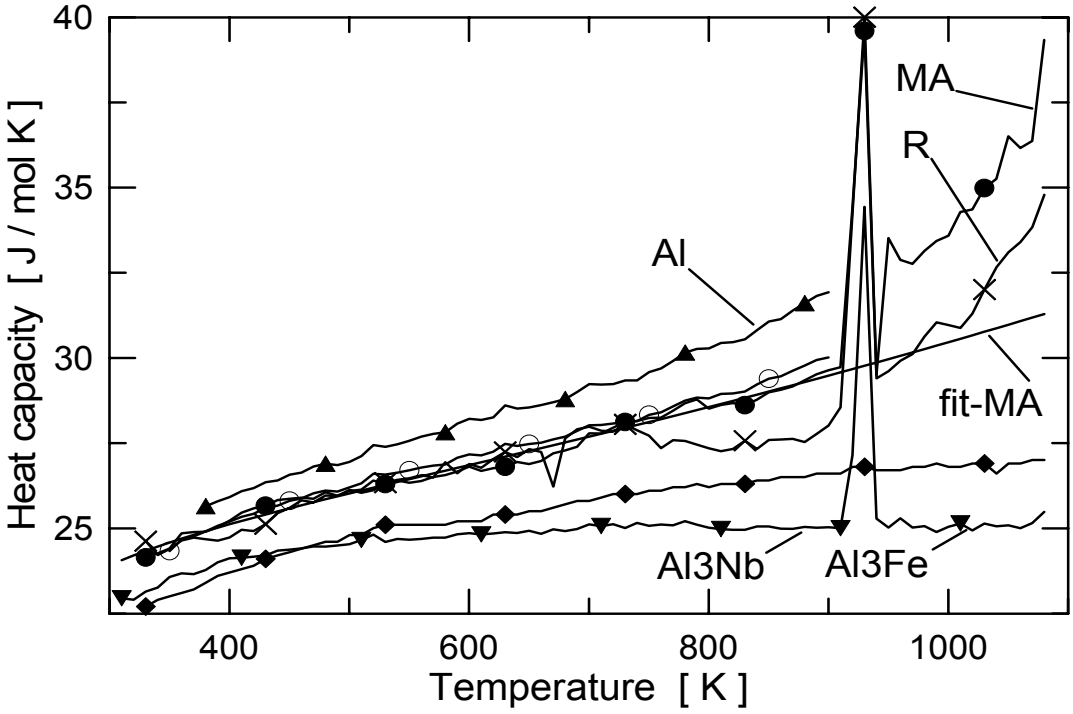

Fig 3 Experimental molar heat capacities (± 1 J mol^{-1} K^{-1}) of α-Al (▲), monoclinic-Al_3Fe (♦), tetragonal-Al_3Nb (▼), relaxed $Al_{90}Fe_7Nb_3$ master alloy (●) and crystallized to 1100 K at 1 K min^{-1} (×) ribbons vs temperature. The theoretically predicted quantities, according to the Neumann-Kopp rule, for $Al_{90}Fe_7Nb_3$ alloy (○). Zig-zag lines connect the experimental data. (Not all data points are shown.) Physically real polynomial (1) fit for the master alloy (——).

Assuming that both the master alloy and the ribbon are mixtures consisting of only three components, the Neumann-Kopp rule states that their heat capacity is the weighted sum of the $C_p(T)$ of the three components

$$1C_{p(Al90Fe7Nb3)} = 0.61C_{p(Al)} + 0.28C_{p(Al3Fe)} + 0.11C_{p(Al3Nb)}. \quad (3)$$

Eq. (3) could also be applied for the theoretical appraisal of the polynomial parameters $a - e$ for the alloy in eq. (1) considering them to be the individual C_p contributions. The experimentally measured data for the master alloy correlate well with the theoretically predicted $C_p(T)$ by eq.(3) and the physically real polynomial (1) fit up to the melting of the first phase as can be seen in Fig.3. However, the heat capacity of the ribbon is insufficient (and this lag even increases after the melting of the Al-rich phase). It might signify that an ineligible part of Al atoms is not in a bulk form accompanying the transition metal elements, which are more uniformly distributed in the ribbon. The relation between the morphology in the master alloy and heat-treated ribbon, as is shown in Fig.4, it confirms.

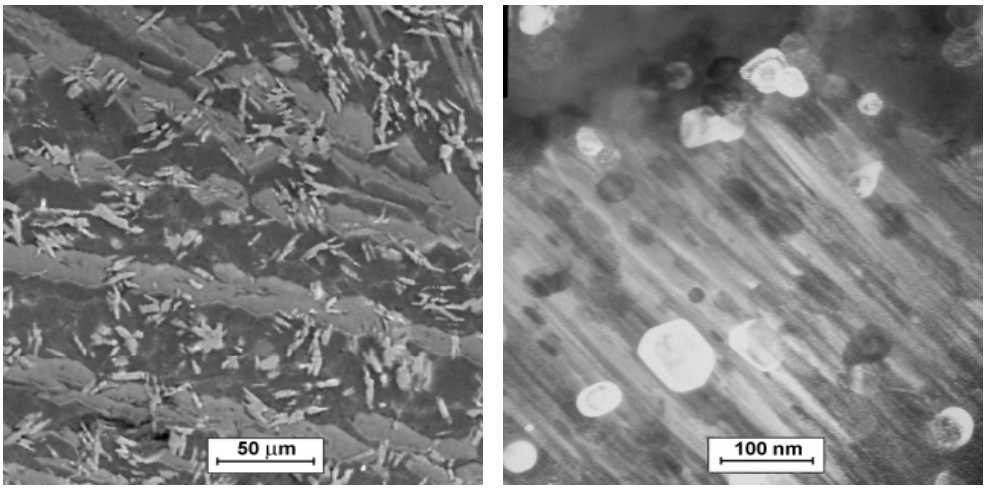

Fig.4 (a) SEM view of $Al_{90}Fe_7Nb_3$ master alloy showing dendrites of Al_3Fe and small grains of Al_3Nb as determined by EDX analysis embedded in polycrystalline Al matrix [5].
(b) TEM view (dark field from diffraction spots close to <200> line of Al) of $Al_{90}Fe_7Nb_3$ ribbon heated to 973 K showing substantially smaller particles of intermetallics Al_3Fe and Al_3Nb embedded in polycrystalline Al matrix [5].

4 Conclusion

The molar heat capacities of the bulk and ribbon $Al_{90}Fe_7Nb_3$ samples as well as their constituent phases have been measured up to 1100 K. The heat capacity of the $Al_{90}Fe_7Nb_3$ master alloy is a sum of heat capacities for its equilibrium Al, Al_3Fe and Al_3Nb phases. However, the Neumann-Kopp rule fails in the case of the $Al_{90}Fe_7Nb_3$ ribbon because of the significant contribution of its Al-Fe and Al-Nb interphases.

Acknowledgement

Authors wish to thank the EC HPRN-CT-2000-00038 project for the financial support.

Table 1 Ideal, theoretically appraised and physically real polynomial coefficients, their standard errors (in %) and reduced chi-square values of the real fits of $C_p(T) = a + bT + cT^2 + dT^{-1} + eT^{-2}$ (in J mol^{-1}K^{-1}) dependence (1) for the α-Al, monoclinic-Al_3Fe, tetragonal-Al_3Nb, relaxed $Al_{90}Fe_7Nb_3$ master alloy and crystallized to 1100 K at 1 K min^{-1} ribbon sample. Fitting range 310 - 1080 K for Al_3Fe and Al_3Nb, 310 – 900 K for Al and master alloy, 310 - 733 K for ribbon

Substance	a [Jmol^{-1} K^{-1}]	$10^4 b$ [J mol^{-1} K^{-2}]	$10^8 c$ [J mol^{-1} K^{-3}]	$10^5 d$ [J mol^{-1}]	$10^{-5} e$ [J mol^{-1} K^{1}]	chi-sq.
Al	24.9	27.00	556.3	5.74*e*	-1.57629	
	24.9	32.54	10.46	5.74*e*		
	24.726	32.54	513.18	5.74*e*	-1.54567	0.0186
	±0.47	const.	±3.21	cons.	±9.30	
Al_3Fe	24.9	32.50	-6.623	8.61*e*	-3.20717	
	24.9	31.36	8.514	8.61*e*		
	24.942	21.70	8.514	8.61*e*	-3.19274	0.0092
	±0.41	±5.07	const.	const.	±3.10	
Al_3Nb	24.9	17.50	-132.1	8.61e	-2.19324	
	24.9	29.48	6.892	8.61*e*		
	25.313	5.000	6.892	8.61*e*	-2.11415	0.0166
	±0.10	±240	const.	const.	±2.88	
Master alloy and ribbon	24.9	12.50	454.2	5.74*e*	-1.57073	
	24.85	25.98	316.2	5.74*e*	-1.84589	
	24.394	25.98	361.4	5.74*e*	-1.39992	0.0350
	±0.64	const.	±6.00	const.	±13.85	

References

[1] Illeková E, Gachon J C, Kuntz J J, Kuhnast F A, 2002 High temperature step by step calorimetry and drop caporimetry of metals, in *Proceedings of Thermophysics 2001*, (Ed. Vozár L, Nitra: Constantine the Philosopher University) pp.13-19

[2] Kraftmakher Y, 1998 Equilibrium vacancies and thermophysical properties of metals, *Physics Reports* **299**, 79-188

[3] Grimvall G, 1999 *Thermophysical properties of materials*, (Amsterdam, Elsevier) pp. 118-184

[4] Illeková E, Švec P, 2002 Vznik a zánik nanokryštalického hliníka v zliatine $Al_{90}Fe_7Nb_3$, in *Proceedings of the 14th Conference of the Czech and Slovak Physicist* in press

[5] Illeková E, Janičkovič D, Kubečka P, Švec P, Gachon J C, 2002 Thermodynamic limitations of the clustering in the $Al_{90}Fe_7Nb_3$ alloy, *Mat. Sci. Eng. A* accepted

[6] Barin I, 1993 *Thermochimical data of pure substances*, 2nd ed. Part 1, (Weinheim, Germany, VCH) p.17

[7] Landolt Börnstein, 1971 *Zaghlenwerte and Functionen aus Physik, Chemie, Astronomie, Geophysik und Technik, Band 2/1 Eigenschaften der materie in Ihren Aggregatzustanden, Mechanisch-Termische Zustandsgrössen, 6. Aufl.*, (Berlin, springer-Verlag) p.438.

[8] Krajčí M, 2002 calculated values by VASP program, *private communication*